CrystEngComm

Accepted Manuscript

ROYAL SOCIETY OF CHEMISTRY

www.rsc.org/crystengcomm

Journal Name

RSCPublishing

ARTICLE

Synthesis, structure determination, and formation of a theobromine:oxalic acid 2:1 cocrystal

Cite this: DOI: 10.1039/xoxxoooooox

Franziska Fischer[a,b], Gudrun Scholz[b], Lisa Batzdorf[a,b], Manuel Wilke[a,b], Franziska Emmerling[a,*]

Received ooth January 2012,
Accepted ooth January 2012

DOI: 10.1039/xoxxoooooox

www.rsc.org/

The structure and the formation pathway of a new cocrystal theobromine:oxalic acid (2:1) is presented. The cocrystal was synthesised mechanochemically and its structure was solved based on the powder X-ray data. The mechanochemical synthesis of this model compound was studied *in situ* using synchrotron XRD. Based on the XRD data details of the formation mechanism could be obtained. The formation can be described as a self-accelerated ('liquid like') process from highly activated species.

Introduction

The properties of active pharmaceutical ingredients (APIs) are typically not optimised for their planned applications.[1-3] This is one of the crucial issues in the development of new pharmaceuticals. Many APIs show insufficient bioavailability, which is closely related to their low water solubility. In addition, the polymorphism of drugs has to be considered. Different modification of a given compound can be formed, due to their similar enthalpies of formation. The crystal structure of a material has a determining influence on its physicochemical properties including melting point, stability against physical and chemical stress, dissolution behaviour, solubility, or bioavailability.[4]

Polymorphs of an API can show a change of the properties or even in the therapeutic effects.[5-7] Therefore, it remains a key challenge to improve the physicochemical properties of a drug. Crystal engineering considerations provide a possibility to overcome this issue.[8] The formation of salts or solvates of APIs are typical approaches to circumvent the problem of low solubility.[9-11] In this context, cocrystals of a given API have gained considerable interest in recent years. Cocrystals are two- or more component crystalline phases consisting of uncharged organic compounds, which interact via intermolecular forces.[2, 12-16] As a result of the cocrystallisation, new crystal structures with new physicochemical properties compared to those of the API emerge.[17-21]

Cocrystals can be synthesised by different methods, typically solution based techniques are used. But these methods imply some disadvantages. For example, the solution based cocrystal formation requires a comparable solubility of the educts for a successful synthesis. Due to the poor solubility of the APIs large amounts of solvent are needed. Additionally, solvent molecules could be incorporated in the crystalline structure of the cocrystal, which complicates the control of the product.[3, 22]

Mechanochemistry is an elegant way to circumvent these problems. Typically no or only small amounts of solvent are needed for the milling reactions. Furthermore, the reactions are very fast, nearly quantitative, and proceed without the formation of by-products. Several cocrystals which were not accessible via conventional methods could only be synthesised mechanochemically.[23-26] Consequently, mechanochemical syntheses have been used increasingly in the past years. A detailed understanding of the underlying mechanism of the mechanochemical syntheses is still scarce.[27, 28] Recently, Friščić *et al*. introduced a real-time and *in situ* monitoring of milling reactions using a mixer mill. These experiments provided the first direct insights in the formation pathways.[29-31] Here, we present first *in situ* XRD study of a milling synthesis using a ball mill setup.

As a model system, a new 2:1 cocrystal of the API theobromine (tb) and the coformer oxalic acid (ox) was used in the milling experiments. The *in situ*-investigation of the reaction was conducted in a Perspex grinding jar using synchrotron XRD. Based on the obtained data, a diffusion mechanism can be postulated.

Results and discussion

The tb:ox cocrystal in the molar ratio of 2:1 was synthesised by neat grinding. In contrary to the structural similar APIs theophylline and caffeine only a few theobromine cocrystals are known.[3, 32, 33] The theobromine:oxalic acid (tb:ox) cocrystal represents an interesting model compound for further investigations of the formation pathway during the mechanochemical syntheses. The powder X-ray diffraction (PXRD) pattern of the new compound is depicted in Fig. 1a in comparison to the PXRD patterns of the reactants tb and ox dihydrate. The powder pattern of the cocrystal shows no contributions of reflections of the reagents, indicating a completed reaction.

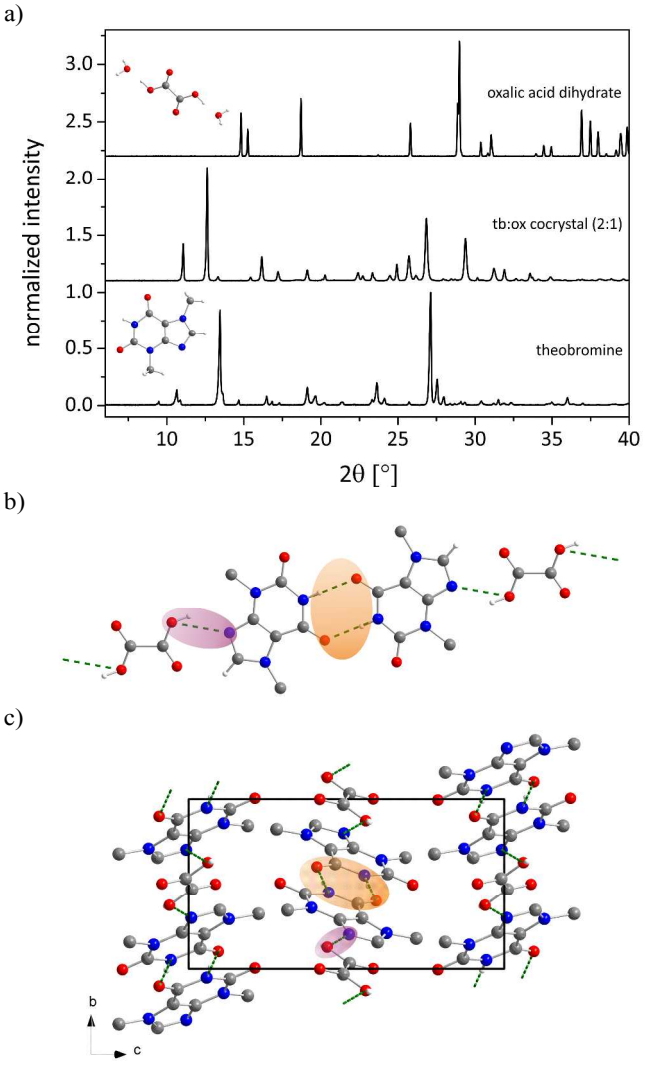

Fig. 1 a) Powder XRD patterns of the tb:ox cocrystal (center) and the reactants theobromine (bottom) and oxalic acid dihydrate (top). The background contributions of the sample holders were corrected. b) bonding arrangement and c) structure of the 2:1 cocrystal tb:ox seen along the *a*-axis. The hydrogen atoms not involved in the hydrogen bonding were omitted for clarity. Green dashed lines indicate hydrogen bonds. b) Structure of the 2:1 cocrystal tb:ox seen along the *a*-axis. The hydrogen atoms not involved in the hydrogen bonding were omitted for clarity. Green dashed lines indicate hydrogen bonds.

Based on the powder pattern a determination of the cocrystal structure followed by a Rietveld refinement was possible. The resulting structure is presented in Fig. 1b. The corresponding Rietveld refinement is shown in Fig. 2 indicating the good agreement between the simulated and measured powder pattern. The tb:ox cocrystal crystallises in the monoclinic space group $P2_1/c$ (a = 8.89209(45) Å, b = 7.50930(28) Å, c = 15.60777(84) Å, β = 116.5691(38)°, V = 932.124(83)Å^3). Each tb molecule is connected to a tb and an ox molecule via hydrogen bonds. One hydrogen bond is formed between the nitrogen atom of the secondary amine of a tb molecule and the oxygen atom from a carbonyl group of another tb molecule (N-H…O, $d_{H...A}$ = 2.803 Å, $d_{D...A}$ = 1.92 Å, $\angle_{D\text{-}H...A}$ = 170°), respectively, resulting in a $\boldsymbol{R_2^2(8)}$ dimer (orange). An additional hydrogen bond (violet) is formed between the tertiary amine of a tb molecule and the hydroxyl group of an ox carboxyl group (O-H…N, $d_{H...A}$ = 2.843 Å, $d_{D...A}$ = 2.12 Å, $\angle_{D\text{-}H...A}$ = 136°), leading to a twisted chain motive running along the *b*-axis.

The absence of water in the crystal structure is evident from the DTA-TGA-measurements (Figure S3). The first DTA signal of the cocrystal arises at a temperature of 252 °C. At this temperature the ox molecules are decomposed. Since the decomposition temperature of ox is 50 K higher than in the pure sample, it can be concluded that the ox molecules are stabilised in the cocrystal.

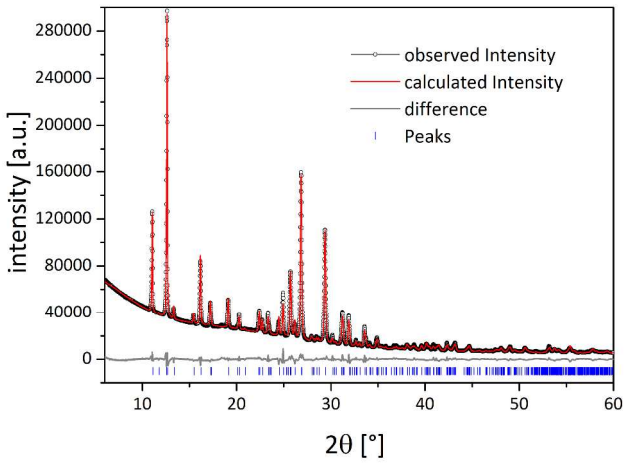

Fig. 2 Rietveld refinement of the crystal structure of the tb:ox cocrystal. Scattered X-ray intensity for the cocrystal tb:ox cocrystal 2:1 at ambient conditions as a function of diffraction angle 2θ. The observed pattern (black circles), the best Rietveld fit profile (red line), the reflection positions (blue tick marks), and the difference curve (grey line) between observed and calculated profiles are shown. The wavelength was λ = 1.54056 Å (Cu-$K_{\alpha1}$). The R-values are R_p = 3.2%, R_{wp} = 4.9%; R_p, and R_{wp} refer to the Rietveld criteria of fit for profile, and weighted profile defined by Langford and Louer.[34]

Based on PXRD data, the position of the hydrogen atoms cannot be determined unambiguously. In order to exclude a salt formation the cocrystal was investigated by Raman (Figure S1) and solid-state NMR (ssNMR) spectroscopy (Figure S2). In the Raman spectra only the band attributed to the carboxylate deformation vibration of ox dihydrate at 478 cm^{-1} shows a pronounced shift.[35] Therefore a protonation of the tb molecules in the cocrystal can be excluded. The strong shift of the carboxylate band indicates that the ox molecules interact much stronger with the water in ox dihydrate than with tb molecule in the cocrystal. This assumption is supported by the ssNMR measurements. The only ssNMR signal, which shifts considerably in the cocrystal, is evoked by the protons of the ox molecules at 17.0 ppm. The shift to 14.2 ppm suggests that the protons of ox are not as strongly bridged in the cocrystal as in pure ox dihydrate. Consequently, it can be assumed that the ox molecules are uncharged in the cocrystal. The water signal at 5.5 ppm disappears in the cocrystal, which reveals that no water molecules are incorporated in the cocrystal. Moreover, the observed line broadening in the ^{1}H MAS NMR spectrum of the cocrystal (Figure S2, middle) supports the assumption of the formation of a network of additional hydrogen bonds.

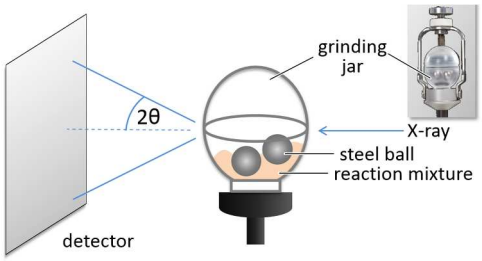

Fig. 3 Experimental setup for collecting the powder patterns during the neat grinding synthesis of the tb: ox cocrystal. The sketch shows a Perspex grinding jar filled with two 10 mm stainless steel grinding balls.

The formation of the cocrystal was observed with *in situ* synchrotron XRD. The *in situ* experiments were conducted at the micro-focus beamline µSpot (BESSY II, Helmholtz Centre Berlin for Materials and Energy, Germany) in transmission geometry using a wavelength of 1.0000 Å. A Perspex grinding jar (Figure 3) was used as reaction vessel. Powder diffraction patterns of the reaction mixture can be measured directly without open the grinding jar.[36] XRD patterns were acquired every 30 s during the milling process.

An investigation of the mechanochemical cocrystal formation pathway is possible since the powder patterns of the cocrystal and the reactants reveal well distinguishable, characteristic reflections. Figure 4 shows the time resolved powder patterns during the neat grinding of tb and ox dihydrate over a time span of 20 minutes. The milling reaction can be divided into three phases. In the first step only the reflections of the reactants tb and ox dihydrate are observed in the XRD patterns (phase 1). In the first 12 min the continuous, slow decomposition of the crystal structure of the reactants proceeds traceable on the basis of the decreasing intensity of the tb reflection at 13.5° (Figure S8). Afterwards the fast formation of the cocrystal proceeds 60 s (phase 2). In this second phase reflections of the reactants are still detectable and decrease quickly with prolonged milling times. Neither the formation of a transient intermediate species nor a prolonged amorphisation of the reaction mixture could be observed during this phase. The last phase begins at a milling time of 13:30 min. At this point there are no crystalline educts detectable in the reaction mixture (phase 3).

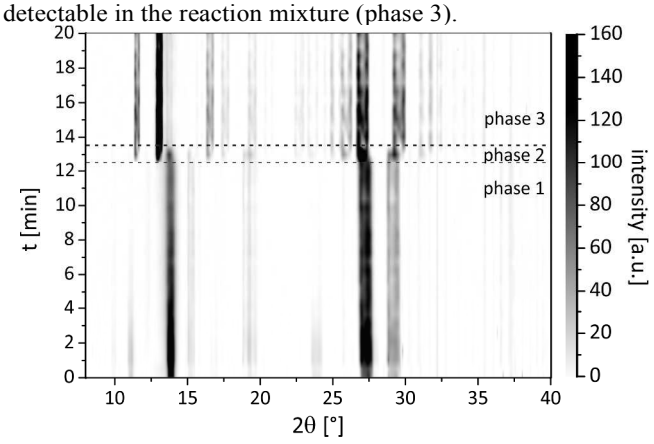

Fig. 4 Time resolved pathway of the powder patterns during the neat grinding synthesis of the tb:ox cocrystal.

Different explanations for mechanochemical reactions are discussed in literature and three theories have to be considered: i) the hot spot theory, ii) the magma-plasma model, and iii) the reaction via diffusion. The hot spot theory is based on the assumption that the attrition between the surfaces causes local temperatures above 1000°C for short periods (10^{-3} - 10^{-4} s) on a molecular dimension.[37-39] The magma-plasma model discusses local temperatures about 10^4 °C leading to transient plasma and the ejection of energy.[37, 40] The third approach emphasises the importance of short diffusion pathways driven by an excellent mixing of the reactants and accelerated reaction.[41] No clear indication for a mechanism based one of the three models could be found for the investigated synthesis. Keeping in mind that the diffusion coefficient in solid state ($D \approx 10^{-16}$ m^2s^{-1}) is significantly lower than the diffusion coefficient in fluid phases ($D \approx 10^{-9}$ m^2s^{-1}) a comparison of the conditions during milling with a liquid-like situation appears obvious.

The fast transformation can be explained by a self-accelerated process from highly activated species completed in 60 s. This process leads to a direct conversion of the solid reactants to the product. There is no driving force based on a salt formation or protonation, since the cocrystal consists only of neutral molecules. The derived formation pathway is illustrated in Figure 5.

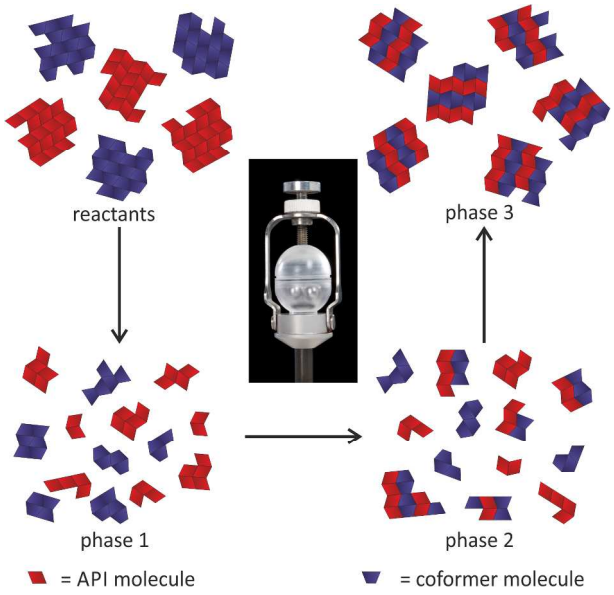

Fig. 5 Representation of the mechanism during the milling synthesis of the 2:1 cocrystal of tb and ox.

Experimental

Materials

Theobromine, $C_7H_8N_4O_2$, (99%, Acros Organics, Belgium) and oxalic acid dihydrate, $C_2H_2O_4 \cdot 2\,H_2O$, (≥ 99+%, Acros Organics, Belgium) were purchased commercially and were used without further purification.

Milling synthesis

The synthesis of the title compound was conducted by neat grinding in a ball mill (MM400, Retsch, Germany) at 30 Hz for 25 min in a molar ratio of 1.9:1 theobromine:oxalic acid dihydrate. A 10 mL steel vessel with two steel balls (10 mm) was used for a total load of 1 g.

XRD measurements

The gained product was investigated by PXRD. The obtained powder pattern did not show any residues of the reagents. All X-ray diffraction experiments were carried out using a D8 diffractometer (Bruker AXS, Karlsruhe, Germany) in transmission geometry (Cu-Kα1 radiation, λ = 1.54056 Å). The structure was solved based on the PXRD pattern using the open source program FOX for indexing and calculating the structure.[42] The program CHEKCELL was used to confirm the unit cell and the space group.[43] FOX uses global-optimisation algorithms to solve the structure by performing trials in direct space. This search algorithm uses random sampling coupled with simulated temperature annealing to locate the global minimum of the figure-of-merit factor. To reduce the total number of degrees of freedom, the theobromine molecule was set rigid. The crystal structure of the cocrystal was solved by the simulated annealing procedure on a standard personal computer within 12h finding the deepest minimum of the cost function several times during the procedure. To complete the structure determination, the structural solution obtained from Monte Carlo/simulated annealing was subsequently subjected to a Rietveld refinement employing the TOPAS software.[44] CSD-1028891 contains the supplementary crystallographic data for the cocrystal tb:ox cocrystal 2:. The data can be obtained free of charge from the Cambridge Crystallographic Data Centre via www.cdc.cam.ac.uk/data_request/cif

Synchrotron measurements

In situ measurements were performed at the micro-focus beamline µSpot (BESSY II, Helmholtz Centre Berlin for Materials and Energy, Germany) in transmission geometry. The powder patterns were collected with a wavelength of 1.0000 Å using a Si (111) double-crystal monochromator. A two-dimensional MarMosaic CCD X-ray detector with 3072x3072 pixels was used to record the scattering intensity. In a typical experiment, XRD patterns were collected for 10 s. The obtained scattering images were processed and converted into diagrams of scattered intensities versus scattering vector q ($q=4\pi/\lambda\sin\theta$) employing an algorithm from the FIT2D software.[45] For the graphical representations, q values were transformed to the diffraction angle 2θ (Cu) to provide a direct comparison to results obtained by XRD experiments performed with Cu radiation. The *in situ* monitoring of the synthesis of the title compound was conducted by neat grinding in mini mill PULVERISETTE 23 (Fritsch, Germany) at 30 Hz for 20 min in a molar ratio of 1.9:1 theobromine:oxalic acid dihydrate. A 10 mL self-constructed Perspex vessel with two steel balls (10 mm) was used for a total load of 1 g. Every 30 s of milling a powder pattern of the sample was taken.

Raman spectroscopy

Raman measurements were performed on a Raman RXN1™ Analyser (Kaiser Optical Systems, France). The spectra were collected using a laser with a wavelength of λ = 785 nm and a contactless probe head (working distance 1.5 cm, spot size 1.0 mm). Raman spectra were recorded with an acquisition time of 5 s and 5 accumulations. NIR excitation radiation at λ = 785 nm and an irradiation of 6.6 W/cm^2 were performed.

ssNMR spectroscopy

^{1}H magic angle spinning (MAS) NMR spectra were recorded on a Bruker AVANCE 400 spectrometer using a 2.5 mm double-bearing MAS probe (Bruker Biospin) and applying a spinning speed of 20 kHz. The ^{1}H MAS NMR spectra were recorded with a π/2 pulse lengths of 3.6 µs, a recycle delay of 5 s and an accumulation number of 256. Existent background signals were suppressed with a phase-cycled depth pulse sequence according to Cory and Ritchey.[46]

DTA and TGA measurements

DTA und TGA measurements were conducted using a thermobalance SETARAM TAG24 in 1600 °C equipment. The measurements were performed in an open Pt jar in a N_2/ synthetic air flow with a heating rate of 10 K/min. No cycle measurements were taken.

Conclusions

The crystal structure of a tb cocrystal with ox in a 2:1 ratio was solved from powder diffraction data. The cocrystal was synthesised mechanochemically. Due to the extremely poor solubility of tb this cocrystal could not be obtained from solution. Based on the Raman spectroscopy and ssNMR data the formation of a salt could be excluded. The synthesis pathway was investigated using *in situ* XRD and a three step mechanism could be derived. The experiment proved that this approach is feasible for the characterisation of mechanochemical reactions.

Acknowledgement

We are grateful to Dr. S. Reinsch (BAM) for DTA-TGA measurements.

Notes and references

[a] BAM Federal Institute for Materials Research and Testing, Richard-Willstaetter-Str. 11, 12489 Berlin, Germany.
E-mail:franziska.emmerling@bam.de.
[b] Department of Chemistry, Humboldt-Universität zu Berlin, Brook-Taylor-Str. 2, 12489 Berlin, Germany.

† Electronic Supplementary Information (ESI) available: DTA-TGA measurements of the reactants and coupled mass spectrometry measurements of the cocrystal. See DOI: 10.1039/b000000x/

References

1. O. Almarsson and M. J. Zaworotko, *Chem Commun*, 2004, 1889-1896.
2. S. Aitipamula, R. Banerjee, A. K. Bansal, K. Biradha, M. L. Cheney, A. R. Choudhury, G. R. Desiraju, A. G. Dikundwar, R. Dubey, N. Duggirala, P. P. Ghogale, S. Ghosh, P. K. Goswami, N. R. Goud, R. R. K. R. Jetti, P. Karpinski, P. Kaushik, D. Kumar, V. Kumar, B. Moulton, A. Mukherjee, G. Mukherjee, A. S. Myerson, V. Puri, A. Ramanan, T. Rajamannar, C. M. Reddy, N. Rodríguez-Hornedo, R. D. Rogers, T. N. G. Row, P. Sanphui, N. Shan, G. Shete, A. Singh, C. C. Sun, J. A. Swift, R. Thaimattam, T. S. Thakur, R. Kumar Thaper, S. P. Thomas, S. Tothadi, V. R. Vangala, N. Variankaval, P. Vishweshwar, D. R. Weyna and M. J. Zaworotko, *Crystal Growth & Design*, 2012, **12**, 2147-2152.

3. H. D. Clarke, K. K. Arora, H. Bass, P. Kavuru, T. T. Ong, T. Pujari, L. Wojtas and M. J. Zaworotko, *Crystal Growth & Design*, 2010, **10**, 2152-2167.
4. N. Schultheiss and A. Newman, *Crystal Growth & Design*, 2009, **9**, 2950-2967.
5. B. Sarma, J. Chen, H. Y. Hsi and A. S. Myerson, *Korean J. Chem. Eng.*, 2011, **28**, 315-322.
6. J. Bauer, S. Spanton, R. Henry, J. Quick, W. Dziki, W. Porter and J. Morris, *Pharm Res*, 2001, **18**, 859-866.
7. J.-P. Brog, C.-L. Chanez, A. Crochet and K. M. Fromm, *RSC Advances*, 2013, **3**, 16905-16931.
8. G. R. Desiraju, *Angewandte Chemie International Edition*, 2007, **46**, 8342-8356.
9. Y. Umeda, T. Fukami, T. Furuishi, T. Suzuki, K. Tanjoh and K. Tomono, *Drug Development and Industrial Pharmacy*, 2009, **35**, 843-851.
10. A. T. M. Serajuddin, *Advanced Drug Delivery Reviews*, 2007, **59**, 603-616.
11. R. Chadha, A. Saini, P. Arora and S. Bhandari, *Critical Reviews in Therapeutic Drug Carrier Systems*, 2012, **29**, 183-218.
12. C. B. Aakeroy, M. E. Fasulo and J. Desper, *Mol Pharm*, 2007, **4**, 317-322.
13. M. C. Etter and G. M. Frankenbach, *Chem Mater*, 1989, **1**, 10-12.
14. T. Friščić and W. Jones, *Journal of Pharmacy and Pharmacology*, 2010, **62**, 1547-1559.
15. C. B. Aakeröy, M. E. Fasulo and J. Desper, *Mol Pharm*, 2007, **4**, 317-322.
16. M. J. Zaworotko, *Crystal Growth & Design*, 2006, **7**, 4-9.
17. D. P. McNamara, S. L. Childs, J. Giordano, A. Iarriccio, J. Cassidy, M. S. Shet, R. Mannion, E. O'Donnell and A. Park, *Pharm Res*, 2006, **23**, 1888-1897.
18. D. J. Good and N. r. Rodríguez-Hornedo, *Crystal Growth & Design*, 2009, **9**, 2252-2264.
19. A. V. Trask, W. D. S. Motherwell and W. Jones, *Int. J. Pharm.*, 2006, **320**, 114-123.
20. A. V. Trask, W. D. S. Motherwell and W. Jones, *Crystal Growth & Design*, 2005, **5**, 1013-1021.
21. N. Chieng, M. Hubert, D. Saville, T. Rades and J. Aaltonen, *Crystal Growth & Design*, 2009, **9**, 2377-2386.
22. J. S. Stevens, S. J. Byard, C. A. Muryn and S. L. M. Schroeder, *J Phys Chem B*, 2010, **114**, 13961-13969.
23. S. L. James, C. J. Adams, C. Bolm, D. Braga, P. Collier, T. Friščić, F. Grepioni, K. D. Harris, G. Hyett and W. Jones, *Chemical Society Reviews*, 2012, **41**, 413-447.
24. D. Braga, L. Maini, M. Polito and F. Grepioni, *Chem Commun*, 2002, 2302-2303.
25. S. Karki, T. Friscic and W. Jones, *Crystengcomm*, 2009, **11**, 470-481.
26. V. R. Pedireddi, W. Jones, A. P. Chorlton and R. Docherty, *Chem Commun*, 1996, 987-988.
27. M. R. Caira, L. R. Nassimbeni and A. F. Wildervanck, *Journal of the Chemical Society, Perkin Transactions 2*, 1995, 2213-2216.
28. M. C. Etter, S. M. Reutzel and C. G. Choo, *J Am Chem Soc*, 1993, **115**, 4411-4412.
29. T. Friščić, I. Halasz, P. J. Beldon, A. M. Belenguer, F. Adams, S. A. J. Kimber, V. Honkimäki and R. E. Dinnebier, *Nat Chem*, 2013, **5**, 66-73.
30. I. Halasz, S. A. J. Kimber, P. J. Beldon, A. M. Belenguer, F. Adams, V. Honkimäki, R. C. Nightingale, R. E. Dinnebier and T. Friščić, *Nat. Protocols*, 2013, **8**, 1718-1729.
31. I. Halasz, A. Puškarić, S. A. J. Kimber, P. J. Beldon, A. M. Belenguer, F. Adams, V. Honkimäki, R. E. Dinnebier, B. Patel, W. Jones, V. Štrukil and T. Friščić, *Angewandte Chemie International Edition*, 2013, **52**, 11538-11541.
32. S. Karki, L. Fábián, T. Friščić and W. Jones, *Organic Letters*, 2007, **9**, 3133-3136.
33. N. Madusanka, M. D. Eddleston, M. Arhangelskis and W. Jones, *Acta Crystallographica Section B*, 2014, **70**, 72-80.
34. J. I. Langford and D. Louer, *Rep. Prog. Phys.*, 1996, **59**, 131-234.
35. Y. Ebisuzaki and S. M. Angel, *Journal of Raman Spectroscopy*, 1981, **11**, 306-311.
36. L. Batzdorf, F. Fischer, M. Wilke, K. J. Wenzel and F. Emmerling, submitted.
37. P. Baláž, in *Mechanochemistry in Nanoscience and Minerals Engineering*, Springer, 2008, pp. 1-102.
38. F. P. Bowden and D. Tabor, *The friction and lubrication of solids*, Clarendon Press, Oxford, 1958.
39. F. P. Bowden and A. D. Yoffe, *The Initiation and Growth of Explosion in Liquids and Solids*, CUP Archive, 1952.
40. P. Thiessen, *Abhandlungen der Deutschen Akademie der Wissenschaften zu Berlin, Klasse für Chemie, Geologie und Biologie*, **1966**, 15.
41. X. Ma, W. Yuan, S. E. J. Bell and S. L. James, *Chem Commun*, 2014.
42. V. Favre-Nicolin and R. Cerny, *Journal of Applied Crystallography*, 2002, **35**, 734-743.
43. J. Laugier and B. Bochu, *Chekcell*, 2001.
44. *Topas Version 2.0, General Profile and Structure Analysis Software for Powder Diffraction Data (User Manual)*, Bruker AXS, Karlsruhe (Germany), 2000.
45. A. P. Hammersley, K. Brown, W. Burmeister, L. Claustre, A. Gonzalez, S. McSweeney, E. Mitchell, J.-P. Moy, S. O. Svensson and A. W. Thompson, *Journal of synchrotron radiation*, 1997, **4**, 67-77.
46. D. G. Cory and W. M. Ritchey, *Journal of Magnetic Resonance (1969)*, 1988, **80**, 128-132.